

The putative cannabinoid receptor GPR55 affects osteoclast function in vitro and bone mass in vivo

Lauren S. Whyte^a, Erik Ryberg^b, Natalie A. Sims^c, Susan A. Ridge^a, Ken Mackie^d, Peter J. Greasley^b, Ruth A. Ross^{a,1,2}, and Michael J. Rogers^{a,1,2}

^aInstitute of Medical Sciences, University of Aberdeen, Aberdeen AB25 2ZD, United Kingdom; ^bAstraZeneca, 43183 Mölndal, Sweden; ^cSt. Vincent's Institute, Fitzroy VIC 3065, Australia; and ^dDepartment of Psychological and Brain Sciences, Indiana University, Bloomington, IN 47401

Edited by L. L. Iversen, University of Oxford, Oxford, United Kingdom, and approved August 3, 2009 (received for review March 17, 2009)

GPR55 is a G protein-coupled receptor recently shown to be activated by certain cannabinoids and by lysophosphatidylinositol (LPI). However, the physiological role of GPR55 remains unknown. Given the recent finding that the cannabinoid receptors CB₁ and CB₂ affect bone metabolism, we examined the role of GPR55 in bone biology. GPR55 was expressed in human and mouse osteoclasts and osteoblasts; expression was higher in human osteoclasts than in macrophage progenitors. Although the GPR55 agonists O-1602 and LPI inhibited mouse osteoclast formation in vitro, these ligands stimulated mouse and human osteoclast polarization and resorption in vitro and caused activation of Rho and ERK1/2. These stimulatory effects on osteoclast function were attenuated in osteoclasts generated from GPR55^{-/-} macrophages and by the GPR55 antagonist cannabidiol (CBD). Furthermore, treatment of mice with this non-psychoactive constituent of cannabis significantly reduced bone resorption in vivo. Consistent with the ability of GPR55 to suppress osteoclast formation but stimulate osteoclast function, histomorphometric and microcomputed tomographic analysis of the long bones from male GPR55^{-/-} mice revealed increased numbers of morphologically inactive osteoclasts but a significant increase in the volume and thickness of trabecular bone and the presence of unresorbed cartilage. These data reveal a role of GPR55 in bone physiology by regulating osteoclast number and function. In addition, this study also brings to light an effect of both the endogenous ligand, LPI, on osteoclasts and of the cannabis constituent, CBD, on osteoclasts and bone turnover in vivo.

bone resorption | CBD | LPI | O-1602 | Rho

A role for the endocannabinoid system (1) in the regulation of bone mass has been demonstrated recently, because mice lacking either of the cannabinoid receptors CB₁ or CB₂ have abnormal bone phenotypes. Furthermore, cannabinoid receptor agonists and inverse agonists reduce bone loss in mice following ovariectomy and have direct effects on both bone-resorbing cells (osteoclasts) and bone-forming cells (osteoblasts) in vitro (2, 3).

In some systems such as the vasculature, there is considerable evidence for a role of non-CB₁/non-CB₂ receptors in mediating some of the effects of certain cannabinoid ligands (for review, see ref. 4). Such non-CB₁/non-CB₂ effects have been observed with a range of cannabinoid ligands including certain endocannabinoids and the phytocannabinoid-like compound O-1602; these effects are antagonized by the cannabis constituent cannabidiol (CBD) (4). Recently, the G protein-coupled receptor GPR55 has been shown to be activated by O-1602 (EC₅₀ = 13 nM) and antagonized by CBD (IC₅₀ = 445 nM) (5–8). In contrast, these compounds have low affinity (5–30 μM) for CB₁ and CB₂ receptors (9, 10). GPR55 also is activated by the bioactive lipid, L-α-lysophosphatidylinositol (LPI) (11, 12).

The physiological role(s) of GPR55 remains unknown. Given the apparent role of CB₁ and CB₂ in regulating bone mass, we examined whether GPR55 is expressed by osteoblasts and osteoclasts and whether this receptor regulates bone cell function in vitro and in vivo. We present evidence that GPR55 plays a role

in bone physiology, with major implications for the development of GPR55- and CBD-related therapeutics.

Results

GPR55 Is Expressed by Osteoclasts. With the use of quantitative PCR, expression of GPR55 mRNA was detected in human osteoclasts generated from macrophage colony-stimulating factor (M-CSF)-dependent monocytes. The mean GPR55 expression was 8-fold higher in osteoclasts than in monocytes in blood from 7 different healthy blood donors (**Supporting Information (SI) Fig. S1A**), and the expression of GPR55 in osteoclasts was similar in males and females; the mean ratio of GPR55:GAPDH expression was 0.096 in 3 male donors, 0.068 in 4 female donors.

GPR55 also was detected as punctuate, vesicular immunofluorescence staining in the cytoplasm and adjacent to the plasma membrane in multinucleated human and mouse osteoclasts (**Figs. S1 B and D and S2A**), in human and mouse primary osteoblasts, and in human TE85 osteoblast-like cells (**Fig. S2 B–D**).

GPR55 Ligands Affect Osteoclast Formation in Vitro. Concentrations of 1 nM to 1 μM O-1602, a GPR55 agonist (13), had no effect on the total number of α_vβ₃-positive osteoclasts generated from human peripheral blood monocytes. However, treatment of cultures with 500 nM of the GPR55 antagonist CBD (6) significantly increased osteoclast number (**Fig. 1A**), similar to the positive control, 10 ng/mL TGF-β (14).

Osteoclasts generated from GPR55^{-/-} bone marrow macrophages (BMMs) appeared larger than wild-type osteoclasts (**Fig. 1D**). Concentrations of 5 nM to 1 μM O-1602 significantly inhibited the formation of multinucleated mouse osteoclasts (**Fig. 1B**), although the macrophages still seemed to differentiate into tartrate-resistant acid phosphatase (TRAP)-positive mononuclear cells (**Fig. 1D**). This inhibitory effect of O-1602 on multinucleated cell formation was not seen in cultures of GPR55^{-/-} BMMs (**Fig. 1B and D**) but still occurred in cultures of CB₁^{-/-} and CB₂^{-/-} BMMs (**Fig. S3**). Furthermore, the inhibitory effect of O-1602 on multinucleated osteoclast formation did not occur in the presence of 500 nM CBD (**Fig. S3**). Like O-1602, the GPR55 ligand LPI also inhibited mouse osteoclast formation, an effect that (as with O-1602) was not seen with GPR55^{-/-} BMMs (**Fig. 1C**).

Author contributions: L.S.W., E.R., N.A.S., S.A.R., P.J.G., R.A.R., and M.J.R. designed research; L.S.W., E.R., N.A.S., and S.A.R. performed research; L.S.W., K.M., and P.J.G. contributed new reagents/analytic tools; L.S.W., E.R., N.A.S., S.A.R., R.A.R., and M.J.R. analyzed data; and L.S.W., E.R., N.A.S., S.A.R., K.M., P.J.G., R.A.R., and M.J.R. wrote the paper.

Conflict of interest statement: E.R. and P.J.G. are employees of AstraZeneca.

This article is a PNAS Direct Submission.

Freely available online through the PNAS open access option.

¹R.A.R. and M.J.R. contributed equally to this work.

²To whom correspondence may be addressed. E-mail: m.j.rogers@abdn.ac.uk or r.ross@abdn.ac.uk.

This article contains supporting information online at www.pnas.org/cgi/content/full/0902743106/DCSupplemental.

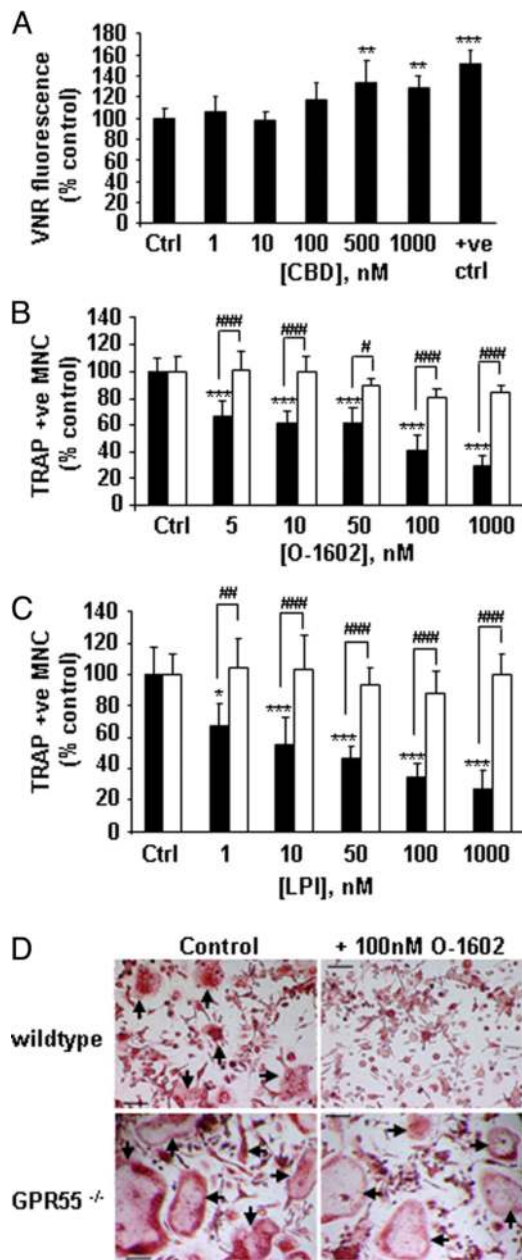


Fig. 1. Effect of GPR55 ligands on human and mouse osteoclast formation. (A) Human monocytes were cultured in the presence of 1 nM to 1 μ M CBD for 7 days and then were fixed and stained for $\alpha_v\beta_3$ (vitronectin receptor, VNR) to quantify osteoclast number. Immunofluorescence intensity was measured and expressed relative to control cultures. Data are mean \pm SEM; $n = 6$ or 7 independent experiments, with 5 replicates for each. ANOVA with Dunnett's post-test; **, $P < 0.01$; ***, $P < 0.001$ compared with control. (B and C) BMMs from wild-type mice (black bar) and GPR55^{-/-} mice (white bar) were cultured in the presence of 5 nM to 1 μ M O-1602 (B) or 1 nM to 1 μ M LPI (C) for 5 days and then were fixed and stained for TRAP. The number of TRAP-positive multinucleated cells (MNCs) was counted and expressed as a percentage of control. Data are mean \pm SEM; $n = 4$ or 5 experiments, 5 replicates for each. ANOVA with Bonferroni post-test; *, $P < 0.05$; ***, $P < 0.001$ compared with control; #, $P < 0.05$; ##, $P < 0.01$; ###, $P < 0.001$ compared with wild type. (D) Representative images of TRAP-positive MNCs (arrowheads) generated from wild-type and GPR55^{-/-} macrophages after treatment with vehicle (control) or 100 nM O-1602. (Scale bar: 50 μ m.)

GPR55 Agonists Stimulate Osteoclast Polarization and Function in Vitro. Treatment of human osteoclasts (cultured on dentine discs for 5 days) with O-1602 caused an increase in the proportion of

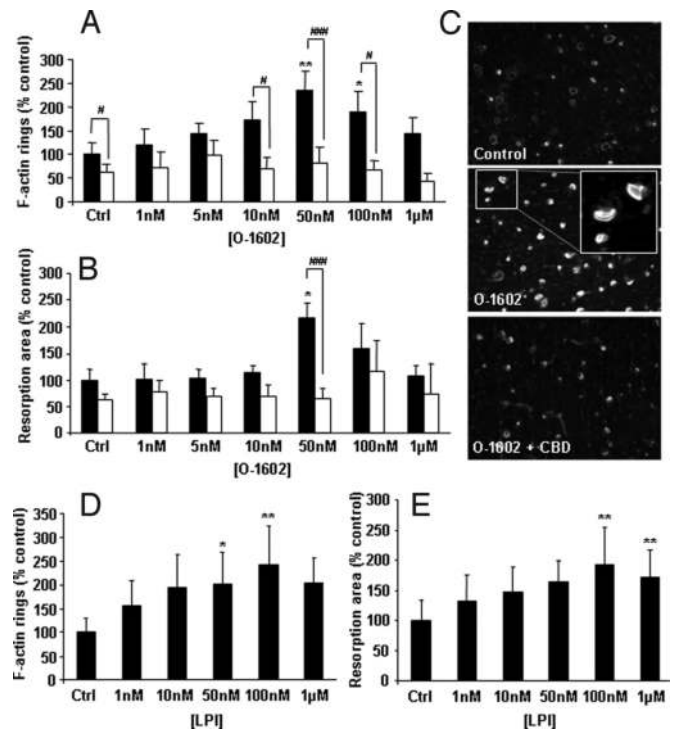


Fig. 2. O-1602 and LPI stimulate human osteoclast polarization and resorption. Human osteoclasts cultured on dentine discs were treated with vehicle (control) or 1 nM to 1 μ M O-1602 with or without 500 nM CBD for 5 days. (A) The number of F-actin rings is expressed as percentage of control cultures \pm SEM. Black bars represent O-1602 alone ($n = 5$ experiments with 5 replicates for each); white bars represent O-1602 + 500 nM CBD ($n = 4$ experiments with 4 or 5 replicates for each). ANOVA with Bonferroni post-test; *, $P < 0.05$; **, $P < 0.01$ compared with control; #, $P < 0.05$; ###, $P < 0.001$ compared with O-1602 alone. (B) Resorption area is expressed as percentage of control \pm SEM. Black bars represent O-1602 alone ($n = 5$ experiments with 5 replicates for each); white bars represent O-1602 + 500 nM CBD ($n = 4$ experiments with 4 or 5 replicates for each). ANOVA with Bonferroni post-test; *, $P < 0.05$ compared with control; ###, $P < 0.001$ compared with O-1602 alone. (C) Representative images of human osteoclasts cultured on dentine, after treatment with vehicle (control), 50 nM O-1602, or 50 nM O-1602 + 500 nM CBD. Cells were stained to visualize polarized cells with F-actin rings (Inset). (D) Human osteoclasts on dentine discs were treated with vehicle (control) or 1 nM to 1 μ M LPI for 5 days. The number of F-actin rings is expressed as percentage of control cultures \pm SEM ($n = 4$ experiments with 4 or 5 replicates for each). ANOVA with Dunnett's post-test; *, $P < 0.05$; **, $P < 0.01$ compared with control. (E) Resorption area is expressed as percentage of control \pm SEM. ($n = 4$ experiments with 3–5 replicates for each). ANOVA with Dunnett's post-test; **, $P < 0.01$.

polarized, actively resorbing osteoclasts with F-actin rings and increased the area of resorption pits on the discs (Fig. 2A–C). Furthermore the GPR55 antagonist CBD, at a concentration of 500 nM (similar to the IC₅₀ value of 445 nM in previous studies) (6), significantly inhibited both the increase in resorption area and the F-actin ring number seen after treatment with 50 nM O-1602 alone ($P < 0.001$) (Fig. 2A–C). This concentration of CBD slightly (but not significantly) reduced the basal level of resorption and significantly decreased the number of polarized osteoclasts with F-actin rings. However, a higher concentration of 1 μ M CBD alone significantly inhibited both human osteoclast polarization and resorption (Fig. S4).

Consistent with the effects seen on human osteoclasts, when mouse osteoclasts were treated with O-1602, we observed a significant increase in the proportion of mouse osteoclasts with F-actin rings (with 1–100 nM O-1602) and a significant increase in resorption area (with 50 nM O-1602) (Fig. S5). LPI, another

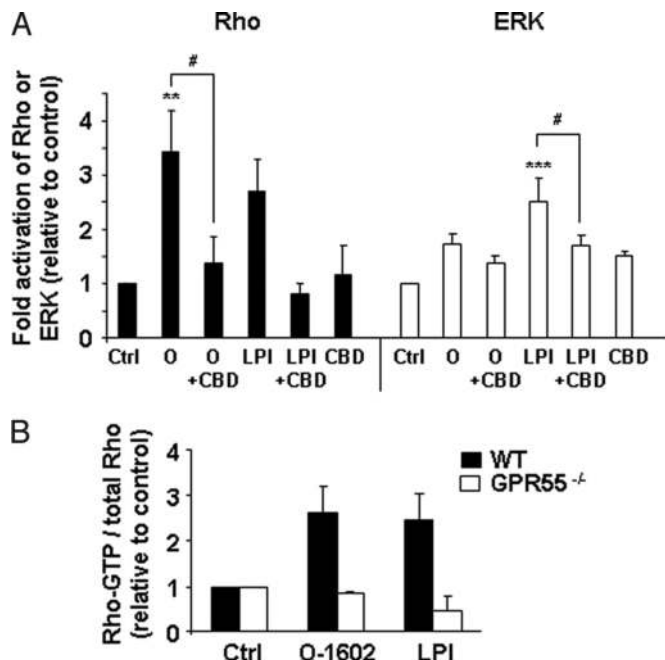


Fig. 3. O-1602 and LPI stimulate Rho activation and ERK phosphorylation in human and mouse osteoclasts. (A) Human osteoclasts were treated with O-1602 (O), LPI, or CBD for 10 min, with or without a 10-min pre-incubation with 1 μ M CBD. Activation of Rho and ERK1/2 was measured on Western blots by densitometry; values are means \pm SEM from 3–7 independent experiments. **, $P < 0.01$; ***, $P < 0.001$ compared with control (Ctrl); #, $P < 0.05$ compared with O-1602 or LPI alone (ANOVA, with Bonferroni post-test). (B) Mouse osteoclasts generated from wild-type macrophages (black bars) or GPR55^{-/-} macrophages (white bars) were starved for 30 min and then were treated as above before measurement of Rho activation ($n = 2$ experiments).

GPR55 agonist, also increased the number of polarized, actively resorbing human osteoclasts (with 100 nM, 242% \pm 82% of control; $P < 0.05$) and increased resorption area (with 100 nM, 192% \pm 61% of control; $P < 0.05$) (Fig. 2 D and E).

O-1602 Activates Rho and ERK Signaling in Osteoclasts. Using a pull-down assay, treatment of human osteoclasts with O-1602 for 10 min caused an increase in active, GTP-bound Rho. This effect was prevented by pretreatment of the osteoclasts for 10 min with 1 μ M of the GPR55 antagonist CBD (Fig. 3A). Although LPI showed the same trend toward Rho activation and inhibition of this effect with CBD, this trend did not reach statistical significance. ERK phosphorylation in human osteoclasts was increased following treatment with LPI; this effect also was prevented by pretreatment with 1 μ M CBD (Fig. 3A). Similarly, O-1602 showed the same trend toward activation of ERK signaling and inhibition of this effect with CBD, but this trend did not reach statistical significance. As with human osteoclasts, treatment of mouse osteoclasts with O-1602 or LPI also caused activation of Rho. This effect was absent in GPR55^{-/-} osteoclasts (Fig. 3B).

O-1602 Has Little Effect on Osteoblast Differentiation. After 72 h, high concentrations of O-1602 in mouse calvarial osteoblasts and HosTe85 cells caused a small but significant decrease in alkaline phosphatase activity, a marker of osteoblast differentiation (Fig. S6A and B). O-1602 at concentrations of 1 nM to 1 μ M had no effect on mineralization in long-term cultures of mouse calvarial osteoblasts (Fig. S6C).

GPR55 Knockout Mice Have Increased Bone Mass. In 12-week-old male GPR55^{-/-} mice, bone volume [bone volume (BV)/tissue

volume (TV)] was significantly increased in the tibia and femur compared with wild-type littermates, together with a significant increase in trabecular number, trabecular connectivity (trabecular pattern factor), and a transition from rod-like to plate-like trabecular structure (structure modulus index) in the femur (Fig. 4 A and B). These changes were not seen in female GPR55^{-/-} mice of the same age. No significant changes in cortical bone volume were detected in male or female mice compared with GPR55^{-/-} mice of the same age.

These differences between male wild-type and male GPR55^{-/-} mice were confirmed by histomorphometric analysis of femoral sections from 12-week-old mice (Table S1). In male, but not female, GPR55^{-/-} mice, trabecular BV/TV was increased significantly, and trabecular separation was reduced significantly compared with male wild-type mice. However, no significant changes were detected in any histomorphometric indices of bone formation, including osteoblast surface, osteoblast number, osteoid surface, osteoid volume, or osteoid thickness.

Male GPR55^{-/-} mice also demonstrated a trebling of osteoclast surface and osteoclast number compared with male wild-type mice. Despite this increase, an impairment in osteoclast function in GPR55^{-/-} animals was confirmed by measurement of cartilage remnants within the trabecular bone, which revealed a doubling of the cartilage content within the trabecular bone of the secondary spongiosa (Fig. 4C and Table S1). Histologically, osteoclasts in GPR55^{-/-} bones appeared plump and inactive. The presence of unresorbed cartilage also was significantly higher in female GPR55^{-/-} mice than female wild-type mice, suggesting a phenotype similar to but milder than that in the male GPR55^{-/-} mice. In contrast to male GPR55^{-/-} mice, however, the number of osteoclasts in female GPR55^{-/-} mice was reduced considerably compared with wild-type mice, and no change in trabecular bone volume was observed.

The GPR55 Antagonist CBD Inhibits Bone Resorption in Vivo. CBD has been estimated to have a half-life of 2–5 days in humans (15, 16). Treatment of male mice for 8 weeks with 10 mg/kg CBD (3 times per week) significantly decreased the level of serum type 1 collagen C-terminal telopeptide fragments (CTX), a biochemical marker of bone resorption, by 18% ($P < 0.05$) (vehicle control = 22.47 ng/L; CBD-treated = 18.27 ng/L). Microtomographic (μ CT) analysis of the proximal tibiae also revealed a trend toward increased BV/TV (+ 10%) and trabecular number (+ 10%), with a decrease in trabecular separation (- 7%), trabecular pattern factor (- 5%), and structure modulus index (- 8%) in the tibia of the CBD-treated mice relative to control. These findings were consistent with a decrease in bone resorption in CBD-treated mice, although these changes were not statistically significant over this treatment schedule.

Discussion

The physiological function of GPR55 is largely unknown. Using immunostaining and quantitative PCR, we demonstrate that both human and mouse osteoclasts and osteoblasts express GPR55 and that GPR55 mRNA is present in human monocytic osteoclast precursors but increases during differentiation into mature, multinucleated osteoclasts. To investigate the role of GPR55 in osteoclast formation, we used a synthetic GPR55 agonist, O-1602 (6, 13). O-1602 significantly inhibited the late stages (including cell fusion) of osteoclastogenesis from mouse precursors. Although there is evidence that O-1602 can act on additional targets (13), in the present study the inhibitory effect of O-1602 on osteoclastogenesis was mediated via GPR55, because this effect was not observed in BMMs from GPR55^{-/-} mice but was retained in macrophages from CB1^{-/-} and CB2^{-/-} mice. Consistent with the inhibitory effect of O-1602 on mouse osteoclast formation in vitro, osteoclast number was significantly higher in the long bones from GPR55^{-/-} mice than in those from

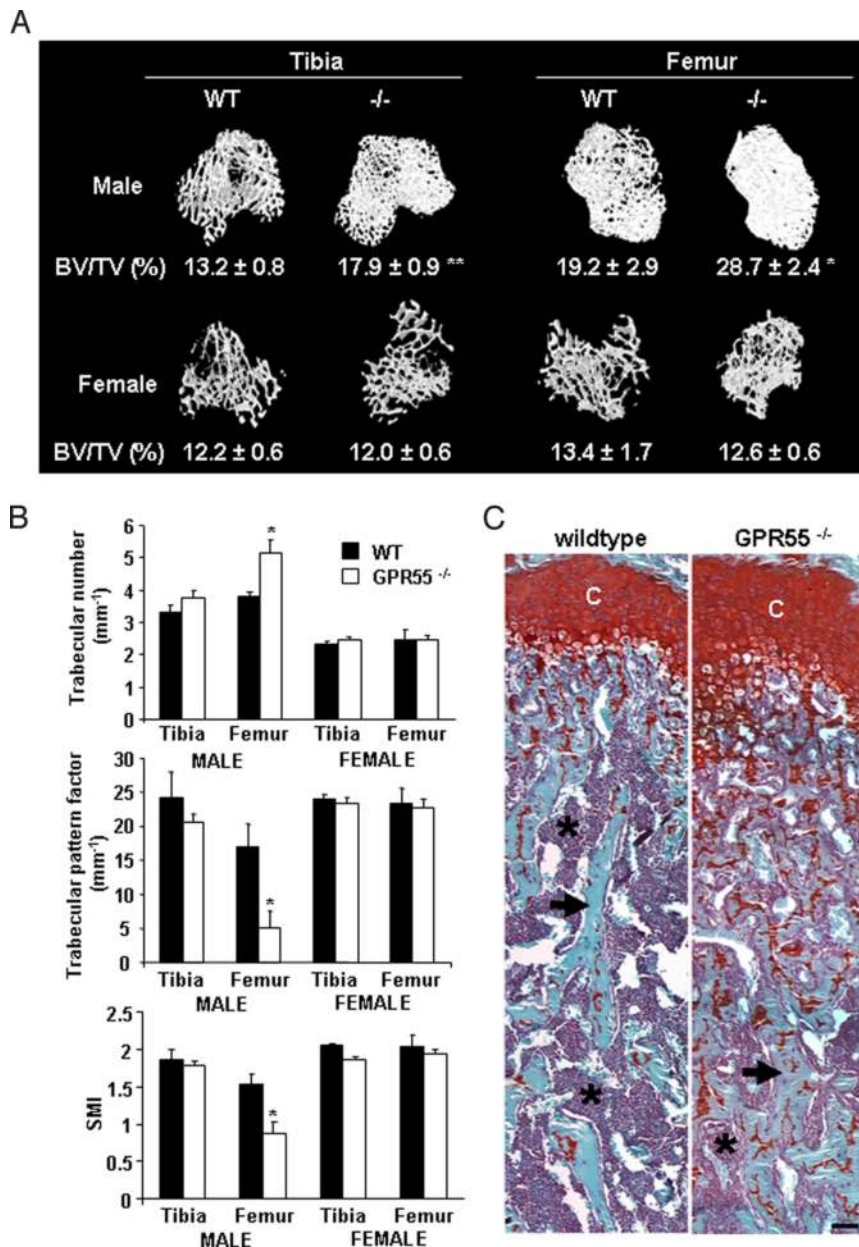


Fig. 4. Trabecular bone volume is increased in male GPR55^{-/-} mice. (A) μ CT reconstructions of trabecular bone in the distal tibial and proximal femoral metaphysis at 12 weeks of age, with mean percent BV/TV values. (B) Significant changes in trabecular number, trabecular pattern factor, and structure modulus index. Black bars indicate wild-type (WT) mice; white bars indicate GPR55^{-/-} mice. Data are mean \pm SEM from 8 wild-type and 4 GPR55^{-/-} male and female mice. Student's *t* test; *, *P* < 0.05; **, *P* < 0.01 compared with wild type. (C) Sections of femora were stained with toluidine blue and Safranin O. Note the increased presence of cartilage remnants (orange) in the trabecular bone (blue) of the GPR55^{-/-} mouse. Asterisks indicate bone marrow (purple); arrows indicate trabecular bone; C, chondrocytes. (Scale bar: 20 μ m).

wild-type mice. O-1602 had no effect on the formation of human osteoclasts *in vitro*. It remains unclear why O-1602 inhibited the formation of mouse osteoclasts but not human osteoclasts; a possibility is that human osteoclasts already produce higher levels of an endogenous agonist. However, consistent with the hypothesis that GPR55 plays some inhibitory role in osteoclastogenesis, the antagonist CBD did increase human osteoclast formation significantly.

Next, we examined the role of GPR55 in osteoclast function. O-1602 had a stimulatory effect on cell polarization and resorption in human osteoclasts that was attenuated in the presence of the GPR55 antagonist CBD. Furthermore, treatment with 1 μ M CBD alone significantly decreased cell polarization and resorp-

tion, presumably by antagonizing the effect of GPR55 ligands present in the culture medium or produced endogenously (such as 2-arachidonoylglycerol, which we recently have shown can be produced by osteoclasts) (17). The endogenous GPR55 agonist LPI also stimulated human osteoclast polarization and resorption. Both O-1602 and LPI elicited a bell-shaped concentration-response relationship for these effects on osteoclasts, a typical response of cultured cells to cannabinoids (18).

The stimulatory effect of GPR55 agonists on osteoclasts probably is mediated, at least in part, by activation of the small GTPase Rho (6, 12, 19), which is known to play important roles in osteoclast polarization and bone resorption (20–22). We found that treatment of human osteoclasts with O-1602 or LPI

caused activation of Rho, an effect that was prevented by pretreatment of osteoclasts with CBD. The stimulatory effect of O-1602 and LPI on Rho was mediated via GPR55, because this effect was absent in mouse osteoclasts derived from GPR55^{-/-} BMMs compared with osteoclasts from wild-type BMMs. LPI (and, to a lesser extent, O-1602) also caused activation of ERK in osteoclasts; ERK is associated with increased osteoclast activity and survival (23–25). Although some studies have failed to show that ERK lies downstream of GPR55 (19), other studies have demonstrated robust GPR55-mediated ERK activation (11, 26). The contradictory nature of these findings may relate to the concept of functional selectivity (27, 28), whereby different signaling pathways (e.g., Rho and ERK) are activated in an agonist- and tissue-specific manner (8). Together, our studies strongly indicate that both Rho and ERK signaling lie downstream of GPR55 in osteoclasts and that GPR55 plays a role in regulating osteoclast function.

Consistent with the stimulatory effects of GPR55 agonists on both human and mouse osteoclast function *in vitro*, male GPR55^{-/-} mice had evidence of decreased bone resorption and an osteopetrotic phenotype. Although osteoclast numbers were increased significantly, osteoclast function was impaired, as indicated by increased cartilage remnants within the trabecular bone (29–31). This impairment in osteoclast function is consistent with our observed effects of O-1602 on osteoclasts *in vitro* and a role for GPR55 in stimulating osteoclast activity. An increase in osteoclast number in the presence of impaired function often is observed in osteopetrotic phenotypes and seems to be a homeostatic response (32).

The reason for the milder bone phenotype in the female GPR55^{-/-} mice is not yet known, because there were no noticeable differences in GPR55 expression in human osteoclasts derived from males or females. It is possible that, *in vivo*, hormonal differences may play a compensatory role in female GPR55^{-/-} mice or that males are more susceptible to loss of GPR55-mediated signaling. Alternatively, this difference could relate to the higher level of remodeling in wild-type female mice compared with males. The high bone mass phenotype of the GPR55^{-/-} mice therefore seems to be predominantly the result of a defect in osteoclast function rather than an increase in osteoblast-mediated bone formation, because O-1602 had little effect on the differentiation or mineralization of osteoblasts cultured *in vitro*, and osteoblast number and osteoblast surface were not altered in the GPR55^{-/-} mice compared with wild-type controls.

Together, our observations indicate that GPR55 has a necessary role in bone physiology, regulating the formation and particularly the activity of osteoclasts. Previous studies have highlighted the involvement of the cannabinoid receptors CB₁ and CB₂ in the local and/or central control of bone mass (2, 3, 33). Opinion is divided as to whether endocannabinoids have the ability to act as agonists of GPR55 (6, 11, 12, 19, 26), but our findings introduce the possibility that the effect of certain endocannabinoids on bone cells may be mediated, at least in part, via GPR55. Lysophospholipids play a role in many physiological and pathophysiological processes and now are recognized as extracellular signaling molecules as well as precursors of phospholipid synthesis (34). We show here that LPI causes activation of ERK and Rho in osteoclasts via GPR55 and hence could play a role in regulating bone resorption *in vivo*.

Our observations also suggest that CBD can inhibit bone resorption *in vivo* via modulation of GPR55 signaling. CBD has been shown to be an effective oral anti-arthritis therapeutic (35). The receptor mechanisms underlying these therapeutic effects of CBD are unknown, but our observations clearly indicate that GPR55 has a role in the pharmacology of CBD. Recently, GPR55^{-/-} mice have been shown to be resistant to neuropathic and inflammatory pain (36); therefore the search for selective GPR55 antagonists for testing in pain models already is under-

way. Our observations suggest that blocking GPR55 also may have direct beneficial effects on bone turnover in arthritic or metabolic bone diseases. Finally, although CBD is a major constituent of cannabis, it remains to be determined whether cannabis smoking may increase bone density, because delta-9-tetrahydrocannabinol, another constituent, also is thought to be a GPR55 ligand (6, 19) and may oppose the effects of CBD.

Methods

Generation and Culture of Osteoclasts. Human osteoclasts were generated from peripheral blood monocytes cultured with 20 ng/mL M-CSF (R&D Systems) and 100 ng/mL receptor activator of NF- κ B ligand (RANKL) (Peprotech EC Ltd) as previously described (37). Samples of whole blood were obtained with informed consent from healthy volunteers with approval from the Local Research Ethics Committee. Monocytes (2×10^5 cells/mL) were treated with O-1602 (Cayman Chemical Co.) or CBD (Tocris Cookson Ltd.) dissolved in DMSO (final concentration 0.1% vol/vol). After 7 days, cells were fixed with 4% paraformaldehyde and stained with 23c6 anti- α v β ₃ (Serotec) and Alexa Fluor 488 goat anti-mouse antibody (Invitrogen). In control cultures, < 1% of the cells were α v β ₃-positive at the start of the culture. Total α v β ₃ immunofluorescence (which showed a significant correlation with the total number of α v β ₃-positive multinucleated cells) was quantified using a BioTek FL600 plate reader.

To study osteoclast polarization and activity, human monocytes were cultured as described earlier on elephant tusk dentine discs for 6 days, treated with O-1602 with or without CBD, with CBD alone, or with LPI (Sigma) for 5 more days, and then were fixed and stained with 0.5 μ g/mL TRITC-phalloidin (Sigma) to visualize F-actin rings (a characteristic cytoskeletal feature of polarized, functionally active osteoclasts) (38, 39). The area of resorbed dentine was quantified as described previously (37).

Mouse osteoclasts were generated by culturing BMMs, from wild-type C57BL/6, CB₁^{-/-} (40), CB₂^{-/-} (3), or GPR55^{-/-} mice, with 50 ng/mL murine M-CSF and 10 ng/mL murine RANKL (R&D Systems), as described previously (41). After 3–5 days with or without O-1602 or LPI, cells were fixed and stained for TRAP (42) to count TRAP-positive multinucleated (≥ 3 nuclei), osteoclast-like cells (MNCs).

To study the activity of mouse osteoclasts, MNCs were generated by coculturing primary osteoblasts (see *Supporting Information*), 1×10^5 cells per well, with bone marrow cells, 1.5×10^6 cells per well, from 3-week-old C57BL/6 mice, on 6-well plates coated with type I collagen (Nitta Gelatin Inc.) in the presence of 10 nM 1 α , 25-dihydroxyvitamin D₃ and 1 μ M prostaglandin E₂. After 6 days the cell population was harvested using 0.1% collagenase (Sigma) and then was seeded onto dentine discs with or without vehicle or 1 nM to 1 μ M O1602 for 48 h. Cells were fixed and stained for F-actin and TRAP before the resorption pit area was quantified as described earlier. The number of F-actin rings per culture was normalized to the number of TRAP-positive MNCs.

Analysis of Rho and ERK Activation. Human and mouse osteoclasts were starved (overnight or for 30 min respectively) of FCS and RANKL/M-CSF and then were treated for 10 min with 1 μ M O-1602, 1 μ M LPI, or 1 μ M CBD (with or without 10-min pretreatment with 1 μ M CBD). Rho-GTP then was quantified in 0.5 mL of cleared cell extract using a Rhotekin pull-down assay according to the manufacturer's instructions (Upstate) using anti-Rho A (26C4) (Santa Cruz Biotechnology) and IR800-labeled anti-mouse (LiCor) antibodies.

To measure ERK activation, human osteoclasts were starved for 4 h and then were treated with O-1602 or LPI (with or without pretreatment with CBD) as described earlier. Fifty μ g of cell lysate were analyzed by Western blotting using anti-phosphorylated ERK1/2 (Cell Signaling Technology #91015) and anti-ERK1/2 (Cell Signaling Technology #9107), followed by Alexa Fluor 688-labeled anti-rabbit (A21076, Invitrogen) and IR800-labeled anti-mouse (LiCor) antibodies. Bands of phosphorylated/total ERK1/2 were visualized simultaneously and quantified using a LiCor Odyssey infrared imager.

Generation of GPR55 Knockout Mice and μ CT Analysis of Long Bones. GPR55 knockout mice were generated by homologous recombination, in which a region containing the complete GPR55 coding sequence in exon 2 was replaced with a loxP-flanked Neo cassette (see *SI Methods*). The GPR55^{-/-} strain was backcrossed 6 generations toward C57BL/6. Mice that were heterozygous for the deletion were intercrossed to produce homozygous GPR55^{-/-} and wild-type littermate control mice. No gross abnormal signs were observed at birth in GPR55^{-/-} animals. Formalin-fixed tibiae and femora from 3-month old mice were scanned using a Skyscan 1072 x-ray Microtomograph at 50 kV/197 μ A. Images were obtained at 5- μ m resolution with a rotation step of 0.67° between each image and were reconstructed using NRecon version 1.4.4 (SkyScan). Trabecular and cortical 2D and 3D morphometric parameters were

analyzed using CTAn version 1.7.0.2 software (SkyScan) and quoted using American Society for Bone and Mineral Research nomenclature.

Histomorphometry. Femora were fixed in 4% buffered formalin/saline (pH 7.4) and were embedded in methyl methacrylate. Longitudinal 1.5- μ m femoral sections were prepared, stained with toluidine blue, and measured by standard histomorphometry in the secondary spongiosa as described previously (43). Safranin O staining was used to detect cartilage remnants within the trabecular bone as described previously (43).

CBD Treatment in Vivo and Serum CTX Measurement. Male C57BL/6 mice were injected i.p. 3 times per week for 8 weeks (infusion rate of 5 μ L/g body weight) with either 10 mg/kg CBD ($n = 5$) or vehicle alone (as a control) ($n = 5$). CBD (Tocris Cookson Ltd) was freshly prepared on each occasion by dissolving CBD in a vehicle of ethanol/cremophor (1:1 vol/vol) and then diluting the solution further in saline until the final solution was ethanol/cremophor/saline, 1:1:18. At the end of the 8-week study, fasted serum samples were collected from individual anesthetized animals, and CTX levels were measured in duplicate

using the RatLaps EIA kit according to the manufacturer's instructions (Immunodiagnostic Systems). Formalin-fixed tibiae and femora from these mice also were analyzed by μ CT as detailed earlier.

Statistics. Data analysis and statistical comparisons were made using 1-way ANOVA or a Students' t test. Following ANOVA, a Dunnett's or Bonferroni post-test was applied to identify significant differences, unless otherwise stated. All analyses were performed on data from at least 3 independent experiments.

ACKNOWLEDGMENTS. We are grateful to Gillian Smith (University of Aberdeen) and Ingrid Poulton (St Vincent's Institute) for assistance with histological processing and to Kevin Mackenzie (University of Aberdeen) for assistance with μ CT analysis. We also thank Dr. Sven Sjögren for his support and acknowledge the excellent technical assistance provided by Anna-Carin Eliasson at Astrazeneca RD Mölndal. This work was supported by a studentship to L.S.W. from the Nuffield Foundation's Oliver Bird Rheumatism Program, by a program grant (17285 to M.J.R.) from the Arthritis Research Campaign, and by the National Institutes of Health Grants DA21696 and DA21285 (to K.M.).

1. Di Marzo V, Bifulco M, De Petrocellis L (2004) The endocannabinoid system and its therapeutic exploitation. *Nature Reviews Drug Discovery* 3:771–784.
2. Idris AI, et al. (2005) Regulation of bone mass, bone loss and osteoclast activity by cannabinoid receptors. *Nat Med* 11:774–779.
3. Ofek O, et al. (2006) Peripheral cannabinoid receptor, CB2, regulates bone mass. *Proc Natl Acad Sci USA* 103:696–701.
4. Begg M, et al. (2005) Evidence for novel cannabinoid receptors. *Pharmacology and Therapeutics* 106:133–145.
5. Baker D, Pryce G, Davies WL, Hiley CR (2006) In silico patent searching reveals a new cannabinoid receptor. *Trends Pharmacol Sci* 27:1–4.
6. Ryberg E, et al. (2007) The orphan receptor GPR55 is a novel cannabinoid receptor. *Br J Pharmacol* 152:1092–1101.
7. Brown AJ (2007) Novel cannabinoid receptors. *Br J Pharmacol* 152:567–575.
8. Ross RA (2009) The enigmatic pharmacology of GPR55. *Trends Pharmacol Sci* 30(3):156–163.
9. Pertwee RG (2007) GPR55: A new member of the cannabinoid receptor clan? *Br J Pharmacol* 152:984–986.
10. Pertwee RG (2008) The diverse CB1 and CB2 receptor pharmacology of three plant cannabinoids: Delta9-tetrahydrocannabinol, cannabidiol and delta9-tetrahydrocannabinol. *Br J Pharmacol* 153:199–215.
11. Oka S, Nakajima K, Yamashita A, Kishimoto S, Sugiura T (2007) Identification of GPR55 as a lysophosphatidylinositol receptor. *Biochem Biophys Res Commun* 362:928–934.
12. Henstridge CM, et al. (2008) The GPR55 ligand L-[alpha]-lysophosphatidylinositol promotes RhoA-dependent Ca2+ signaling and NFAT activation. *FASEB J* 23:183–193.
13. Johns DG, et al. (2007) The novel endocannabinoid receptor GPR55 is activated by atypical cannabinoids but does not mediate their vasodilator effects. *Br J Pharmacol* 152:825–831.
14. Quinn JM, et al. (2001) Transforming growth factor beta affects osteoclast differentiation via direct and indirect actions. *J Bone Miner Res* 16:1787–1794.
15. Ohlsson A, et al. (1986) Single-dose kinetics of deuterium-labelled cannabidiol in man after smoking and intravenous administration. *Biomed Environ Mass Spectrom* 13:77–83.
16. Consroe P, Kennedy K, Schram K (1991) Assay of plasma cannabidiol by capillary gas chromatography/ion trap mass spectroscopy following high-dose repeated daily oral administration in humans. *Pharmacol Biochem Behav* 40:517–522.
17. Ridge SA, Ford L, Cameron GA, Ross RA, Rogers MJ (2007) Endocannabinoids are produced by bone cells and stimulate bone resorption in vitro. *Bone (NY)* 40 (Suppl1): S120.
18. Paton WD, Pertwee RG (1973) *The Pharmacology of Cannabis in Man. Marijuana: Chemistry, Pharmacology, Metabolism and Clinical Effects* (Academic, New York), pp 287–333.
19. Lauckner JE, et al. (2008) GPR55 is a cannabinoid receptor that increases intracellular calcium and inhibits M current. *Proc Natl Acad Sci USA* 105:2699–2704.
20. Coxon FP, Rogers MJ (2003) The role of prenylated small GTP-binding proteins in the regulation of osteoclast function. *Calcif Tissue Int* 72:80–84.
21. Chellaiiah MA, et al. (2000) Rho-A is critical for osteoclast podosome organization, motility, and bone resorption. *J Biol Chem* 275:11993–12002.
22. Zhang D, et al. (1995) The small GTP-binding protein, rho p21, is involved in bone resorption by regulating cytoskeletal organization in osteoclasts. *J Cell Sci* 108:2285–2292.
23. Bradley EW, Ruan MM, Oursler MJ (2008) Novel pro-survival functions of the Kruppel-like transcription factor Egr2 in promotion of macrophage colony-stimulating factor-mediated osteoclast survival downstream of the MEK/ERK pathway. *J Biol Chem* 283:8055–8064.
24. Nakamura H, Hirata A, Tsuji T, Yamamoto T (2003) Role of osteoclast extracellular signal-regulated kinase (ERK) in cell survival and maintenance of cell polarity. *J Bone Miner Res* 18:1198–1205.
25. Miyazaki T, et al. (2000) Reciprocal role of ERK and NF-kappaB pathways in survival and activation of osteoclasts. *J Cell Biol* 148:333–342.
26. Waldeck-Weiermair M, et al. (2008) Integrin clustering enables anandamide-induced Ca2+ signaling in endothelial cells via GPR55 by protection against CB1-receptor-triggered repression. *J Cell Sci* 121:1704–1717.
27. Mailman RB (2007) GPCR functional selectivity has therapeutic impact. *Trends Pharmacol Sci* 28:390–396.
28. Bosier B, Hermans E (2007) Versatility of GPCR recognition by drugs: From biological implications to therapeutic relevance. *Trends Pharmacol Sci* 28:438–446.
29. Sims NA, et al. (2002) Deletion of estrogen receptors reveals a regulatory role for estrogen receptors-beta in bone remodeling in females but not in males. *Bone (NY)* 30:18–25.
30. Sims NA, et al. (2005) Interleukin-11 receptor signaling is required for normal bone remodeling. *J Bone Miner Res* 20:1093–1102.
31. Walker EC, et al. (2008) Cardiotrophin-1 is an osteoclast-derived stimulus of bone formation required for normal bone remodeling. *J Bone Miner Res* 23:2025–2032.
32. Sims NA, Gooi JH (2008) Bone remodeling: Multiple cellular interactions required for coupling of bone formation and resorption. *Seminars in Cell Development Biology* 19:444–451.
33. Tam J, et al. (2008) The cannabinoid CB1 receptor regulates bone formation by modulating adrenergic signaling. *FASEB J* 22:285–294.
34. Falasca M, et al. (1995) Signalling pathways involved in the mitogenic action of lysophosphatidylinositol. *Oncogene* 10:2113–2124.
35. Malfait AM, et al. (2000) The nonpsychoactive cannabis constituent cannabidiol is an oral anti-arthritis therapeutic in murine collagen-induced arthritis. *Proc Natl Acad Sci USA* 97:9561–9566.
36. Staton PC, et al. (2008) The putative cannabinoid receptor GPR55 plays a role in mechanical hyperalgesia associated with inflammatory and neuropathic pain. *Pain* 139:225–236.
37. Sobacchi C, et al. (2007) Osteoclast-poor human osteopetrosis due to mutations in the gene encoding RANKL. *Nat Genet* 39:960–962.
38. Lakkakorpi PT, Vaananen HK (1991) Kinetics of the osteoclast cytoskeleton during the resorption cycle in vitro. *J Bone Miner Res* 6:817–826.
39. Saltel F, Chabadel A, Bonnelye E, Jurdic P (2008) Actin cytoskeletal organisation in osteoclasts: A model to decipher transmigration and matrix degradation. *Eur J Cell Biol* 87:459–468.
40. Tam J, et al. (2006) Involvement of neuronal cannabinoid receptor CB1 in regulation of bone mass and bone remodeling. *Mol Pharmacol* 70:786–792.
41. Takahashi N, Udagawa N, Tanaka S, Suda T (2003) Generating murine osteoclasts from bone marrow. *Bone Research Protocols*, eds Helfrich MH, Ralston SH (Humana Press, Totowa, NJ), pp 129–144.
42. van't Hof RJ (2003) Osteoclast formation in the mouse coculture assay. *Bone Research Protocols*, eds Helfrich MH, Ralston SH (Humana Press, Totowa, NJ), pp 145–152.
43. Sims NA, Brennan K, Spaliviero J, Handelsman DJ, Seibel MJ (2006) Perinatal testosterone surge is required for normal adult bone size but not for normal bone remodeling. *Am J Physiol* 290:E456–E462.